Journal of Comparative Physiology B (2021) 191:85–98
https://doi.org/10.1007/s00360-020-01320-2

ORIGINAL PAPER

A marine teleost, *Opsanus beta*, compensates acidosis in hypersaline water by H^+ excretion or reduced HCO_3^- excretion rather than HCO_3^- uptake

Zongli Yao[1,2] · Kevin L. Schauer[2] · Ilan M. Ruhr[2,4] · Edward M. Mager[2,3] · Rachael M. Heuer[2] · Martin Grosell[1,2]

Received: 10 February 2020 / Revised: 10 September 2020 / Accepted: 29 September 2020 / Published online: 17 October 2020

Abstract

Increases in ambient salinity demand parallel increases in intestinal base secretion for maintenance of osmoregulatory status, which is likely the cause of a transient acidosis following transfer of euryhaline fish from freshwater to seawater. It was predicted that transfer of the marine Gulf toadfish (*Opsanus beta*) from seawater (35 ppt) to hypersaline (60 ppt) seawater (HSW) would lead to a transient acidosis that would be compensated by increases in branchial acid excretion to offset the acid–base disturbance. Toadfish exposed to HSW showed a significant decrease in blood pH and [HCO_3^-] but no increase in pCO_2, followed by a full recovery after 48–96 h. A similar metabolic acidosis and recovery was found when fish were exposed to 60-ppt HCO_3^--free seawater (HEPES-buffered), which may suggest that compensation for intestinal base loss during hypersaline treatment is from gill H^+ excretion rather than gill HCO_3^- uptake. However, we cannot rule out that reduced branchial HCO_3^- excretion contributed to an increase in net acid excretion. Since colchicine prevents full compensation, translocation of H^+ and/or HCO_3^- transporters between cytosolic compartments and plasma membrane fractions might be involved in compensating for the hypersalinity-induced acidosis. Translocation of transporters rather than de novo synthesis may represent a faster and less energetically demanding response to rapidly fluctuating and high salinities encountered by toadfish in their natural environment.

Keywords H^+ excretion · H^+-ATPase · Osmoregulation · Metabolic acidosis · Hypersaline water

Introduction

Marine teleosts are osmoregulators, maintaining extracellular fluids at approximately one-third strength (300–350 mOsm) of seawater. As a consequence, they are faced with constant diffusive water loss to their concentrated seawater environment (Grosell and Taylor 2007). To cope with this hypersaline environment, fish must continually drink seawater and perform NaCl-coupled water absorption in the intestine (Larsen et al. 2014). At the same time, they secrete high rates of HCO_3^- to form $CaCO_3$ precipitates in the intestine, which reduces luminal osmolality, further aiding water absorption (Grosell 2011).

Precipitation of $CaCO_3$ in the Gulf toadfish (*O. beta*) intestine is facilitated by the anion exchanger SLC26a6, which excretes two or more molecules of HCO_3^- in exchange for a single Cl^-, across the apical membrane (Genz et al. 2008; Grosell 2006, 2011; Kurita et al. 2008). While this process is essential for osmoregulation in marine environments, the secretion of HCO_3^- generates protons that

Communicated by B. Pelster.

Electronic supplementary material The online version of this article (https://doi.org/10.1007/s00360-020-01320-2) contains supplementary material, which is available to authorized users.

✉ Zongli Yao
yaozl@ecsf.ac.cn

[1] Sino-US joint laboratory of Aquatic Animal Physiology, East China Sea Fisheries Research Institute, Chinese Academy of Fisheries Sciences, Shanghai, China

[2] Department of Marine Biology and Ecology, Rosenstiel School of Marine and Atmospheric Science, University of Miami, Miami, FL, USA

[3] Department of Biological Sciences, University of North Texas, Denton, TX, USA

[4] Cardiovascular Sciences, School of Medical Sciences, The University of Manchester, Manchester, UK

are transported from intestinal cells to the blood (Cooper et al. 2010; Genz et al. 2008). Consequently, it seems reasonable to expect that changes in intestinal base secretion rates, as seen during exposure to elevated environmental salinity (Genz et al. 2008; Gonzalez 2012; Ruiz-Jarabo et al. 2017), would have an impact on whole-animal acid–base balance. Indeed, most studies on euryhaline fish transferred from freshwater to seawater report a transient acidosis (Maxime et al. 1991; Nonnotte and Truchot 1990; Wilkes and Mcmahon 1986) that is likely due to the onset of drinking and intestinal base secretion (Grosell 2010). Two studies have shown no apparent effect on blood acid–base status following transfer to seawater (Bath and Eddy, 1979; Milne and Randall 1976), while one has shown a transient alkalosis (Perry and Hemin 1981). Considering the need for elevated intestinal HCO_3^- secretion that is generally observed in marine teleosts when transferred from seawater to elevated salinity (Genz et al. 2008), we tested the response of Gulf toadfish transferred from seawater (35 ppt) to hypersaline (60 ppt) seawater (HSW), and predicted that they would experience a similar acidosis, as described above. Since Gulf toadfish readily cope with salinities up to 60 ppt, we further predicted that an acidosis induced by a transfer to HSW would be transient in nature and ultimately corrected by increased net branchial acid excretion, as reported previously (Genz et al. 2008).

Because the aqueous medium limits respiratory compensation for regulating acid–base status, fish rely mainly on the exchange of acid–base equivalents (e.g., H^+ and HCO_3^-) between the gill and the environment (Evans et al. 2005). Correction of a metabolic acidosis resulting from elevated intestinal base secretion could occur through multiple branchial pathways including: (1) uptake of HCO_3^- from the surrounding medium, as suggested for Gulf toadfish (Esbaugh et al. 2012) during CO_2 exposure; (2) reduced HCO_3^- excretion; (3) from regulation of proton transport via Na^+/H^+ exchangers (NHEs) (Catches et al. 2006); or (4) by translocation of proton pumps from cytosolic compartments to plasma membranes, as seen in elasmobranchs (Tresguerres et al. 2006).

It is well established that fish transferred to high salinity show elevated branchial Na^+/K^+-ATPase (NKA) activity to maintain Na^+ and Cl^- excretion and, possibly, acid–base balance (Guffey et al. 2011). Furthermore, cytosolic carbonic anhydrase activity has been reported to increase in the gills upon transfer to elevated salinity in Gulf toadfish, pointing to increased transfer of acid–base equivalents (Sattin et al. 2010). The roles of NHEs and vacuolar H^+-ATPase (VHA) in acid excretion, associated with osmoregulation at elevated salinities, are still unclear. Earlier work on Gulf toadfish revealed that mRNA expression and protein activity of VHA did not change following transfer to elevated salinity (Guffey et al. 2011). However, studies on elasmobranchs have shown that branchial responses to acid–base balance disturbances involve the translocation of the mature VHA protein, rather than changes in mRNA or protein expression (Tresguerres et al. 2006).

NHEs have been proposed as another important mode of controlling acid excretion in seawater fish, where the high ambient Na^+ concentration of seawater favors Na^+ entry across the apical membrane, resulting in excretion of H^+ ions (Claiborne et al. 2002; Liu et al. 2016), as well as ammonia excretion (Liu et al. 2013).

Considering the four compensatory pathways involved during hypersaline exposure, the present study examined if the observed correction of a transient acidosis following transfer to elevated salinity was due to HCO_3^- uptake or H^+ excretion. Moreover, given that we observed a lack of reliance on ambient HCO_3^- for correction of a metabolic acidosis, we hypothesized that altered expression of NHEs, translocation of VHA, or both play a role in enhanced acid excretion during exposure to elevated salinity.

Materials and methods

Experimental animals

Gulf toadfish (*O. beta*) were obtained from local shrimp fishermen in Biscayne Bay, FL, USA. Animals were separated by size, placed in 62-l tanks (8–10/tank), with a continuous flow-through of filtered seawater from Biscayne Bay (34–36 ppt salinity, 22–25 °C). Shelters of polyvinyl chloride tubing were provided to reduce stress and aggression, and fish were fed weekly with squid to satiation. Food was withheld at least 72 h before experimentation to avoid post-prandial acid–base balance disturbances. Fish husbandry and experimental procedures were performed according to an approved University of Miami Animal Care Protocol (Institutional Animal Care and Use Committee iNo. 13-225).

Cannulation experiments

Toadfish (mass: 80–110 g) were exposed to 0.2 g/l MS-222 (buffered with 0.3 g/l $NaHCO_3$) in seawater until anesthetized, and gills were irrigated with 0.1 g/l MS-222 (buffered with 0.3 g/l $NaHCO_3$) seawater throughout surgery. A caudal incision under the lateral line allowed for insertion of a catheter of polyethylene tubing (PE50; Intramedic, Becton–Dickinson & Co., Sparks, MD, USA) into the caudal artery or vein. The catheter was enclosed in a short sleeve of larger tubing (PE90) secured to the skin by surgical suture, anchoring the catheter. The caudal incision was treated with antibiotic (oxytetracycline) before being closed with a surgical suture running stitch. Prior to cannulation, the catheter was filled with heparinized saline (Genz et al. 2008)

and sealed. Cannulated animals were placed in individual holding tanks (approximately 750 ml) with numerous holes (2 cm diameter) and placed in a large bath of aerated, temperature-controlled control seawater.

Blood pH during hypersaline transfer

A total of four experimental groups (Table 1) were subjected to blood pH measurements. In addition to controlling fish held in normal seawater of 35 ppt (SW), there were three treatment groups: those held in hypersaline water of 60 ppt (HSW), unbuffered HCO_3^--free hypersaline water of 60 ppt (UHSW), and HEPES-buffered HCO_3^--free hypersaline water of 60 ppt (BHSW). The HEPES-buffered HCO_3^--free seawater treatment was included since the UHSW treatment resulted in an unexpected respiratory acidosis. HSW water was made by adding sea salt (Instant Ocean; Aquarium Systems Inc., Mentor, OH, USA) to 35-ppt seawater (SW) to a final salinity of 60 ppt. UHSW was made by dissolving the following salts in reverse osmosis water (RO water): 845.3 mmol/l NaCl, 60.9 mmol/l $MgSO_4$, 39.4 mmol/l MgCl2, 14.5 mmol/l KCl, 20.4 mmol/l $CaCl_2$, 4.2 mmol/l Na-gluconate. BHSW was made from UHSW by adding 4.2 mmol/l HEPES and the pH was adjusted to 8.04. Toadfish experience salinities as high as 60 ppt in their natural environment (Kelble et al. 2007). We acknowledge that our "HCO_3^--free" media must have contained some HCO_3^-. However, similar HCO_3^--free artificial seawaters have been employed in studies of toadfish compensatory responses to elevated CO_2. These studies demonstrated that the low HCO_3^- levels in our "HCO_3^--free" media were sufficiently low to reveal dependence of external HCO_3^- (Esbaugh et al. 2012).

Table 1 Water composition and chemistry of four treatments

Chemicals (mM)	SW	HSW	UHSW	BHSW
NaCl	422.66	845.31	845.31	845.31
$MgSO_4$	30.43	60.85	60.85	60.85
$MgCl_2$	19.68	39.35	39.35	39.35
KCl	7.24	14.49	14.49	14.49
$CaCl_2$	10.20	20.41	20.41	20.41
$NaHCO_3$	2.10	4.20	0.00	0.00
Na-gluconate			4.20	0.00
HEPES salt			0.00	4.20
pH	7.89	7.80	7.59	7.91
Osmolality (mOsmol/L)	1136	1913	1907	1912
Water temperature (°C)	24.46	24.46	24.46	24.46

SW seawater, *HSW* 60-ppt hypersaline water, *UHSW* 60-ppt HCO_3^--free hypersaline water, *BHSW* 60-ppt HEPES-buffered HCO_3^-free hypersaline water

Following a post-surgery recovery period of 24 h, water in the containers holding the fish was exchanged from SW to either SW, HSW, UHSW, or BHSW, according to the assigned treatment group. Blood was sampled (~ 380 µl, $n = 8$) via the caudal catheter into a gas-tight heparinized Hamilton syringe at 15 min, 30 min, 1 h, 2 h, 4 h, 8 h, 24 h, 48 h, 72 h, and 96 h, after a daily 50% water replacement. Blood pH was analyzed immediately after sampling, using a Radiometer pHc4000-8 electrode housed in a custom-made, gas-tight chamber. The remaining blood was centrifuged for 1 min to separate the red blood cells and plasma. The plasma was analyzed for total CO_2 and osmolality. Following sampling, the red blood cells were resuspended in 200 µl heparinized saline and was injected back into the fish via the caudal catheter to ensure sustained red blood cell levels.

Colchicine treatment

A fifth experimental series, and corresponding control, examined the role of intracellular trafficking of transport proteins in compensation for hypersaline-induced metabolic acidosis by injection of colchicine, an inhibitor of microtubule polymerization and, consequently, intracellular translocation. A colchicine stock solution (10 mg/ml) in heparinized saline was made just prior to injection. Following a post-surgery recovery period of 24 h, fish ($n = 8$) were injected with a bolus dose of 15 mg/kg of colchicine, while control fish ($n = 8$) were injected with an equivalent volume of saline at $t = 0$ through the caudal catheter. The chosen colchicine concentration showed inhibition of H^+-ATPase translocation in the H^+-ATPase-rich cell in previous studies (Tresguerres et al. 2006). Because colchicine has a half-life in plasma of ~ 1 h, the protocol by Gilmour et al. (1998) and Tresguerres et al. (2006) of injecting half the initial dose every 6 h (at 6 h, 12 h, 18 h, 24 h) was followed. The same injections of saline were performed in corresponding controls. Blood was sampled (~ 380 µ) via the caudal catheter at 15 min, 30 min, 1 h, 2 h, 4 h, 8 h, 24 h from both experimental groups after replacement of SW medium with HSW. Sampled blood was treated as outlined above.

mRNA expression and localization of acid–base relevant proteins during hypersaline transfer

To analyze the mRNA expression and localization of acid–base relevant proteins, a separate experiment was conducted. Toadfish (mass: 20–30 g, $n = 8$) were acutely transferred from SW to HSW for 168 h. Gills were sampled at 0 h, 6 h, 12, 24 h, 96 h, and 168 h after exposure to HSW. Toadfish were euthanized by immersion in a solution of 0.2 g/l MS-222 (buffered with 0.3 g/l $NaHCO_3$) in SW or BHSW as appropriate. The gills were perfused with heparinized saline to clear tissues of blood prior to dissection.

Perfusion methods were performed according to the study of Esbaugh et al. (2005) by exposing and cannulating the bulbus arteriosus with polyethylene tubing (PE50) and using a peristaltic pump to deliver 20 ml of ice-cold heparinized 0.9% saline (50·I.U./ml sodium heparin), followed by 30 ml of non-heparinized saline. Immediately after cannulating the bulbus arteriosus, the ventricle was severed to allow fluid to drain from the circulatory system. Gill tissues for mRNA expression and western blot analyses were immediately snap-frozen in liquid N_2, and stored at − 80 °C until analysis. Gill segments for immunohistochemistry analysis were fixed in Z-fix (Anatech), a formaldehyde-based fixative designed to reduce cross-linking for at least 48 h while gill segments for transmission electron microscopy were fixed in 2% glutaraldehyde buffered with 0.1 mol/l sodium cacodylate (pH = 7.4; osmolality of fixative = 351) at 4 °C overnight.

Analytical techniques

Molecular biology

Total RNA was isolated from toadfish gill using RNA Stat-60 Reagent (Tel-test Inc, TX, USA) according to the manufacturer's instructions, with homogenization performed using a motor-driven tissue homogenizer. The purity of RNAs were determined by measuring 230, 260, and 280-nm absorbance on a SpectraMax Plus 384 Microplate Reader (Molecular Devices, CA, USA). Only RNAs with an absorbance ratio A260/A280 greater than 1.8 were used in further experiments. Prior to cDNA synthesis, a subsample of RNA was DNase treated with amplification grade DNase I (Invitrogen, CA, USA; manufacturer specifications) to remove potential DNA contamination. Subsequent cDNA synthesis was performed using RevertAid MULV reverse transcriptase (Fermentas, MD, USA) according to the manufacturer's specifications.

Real-time PCR amplification and detection were performed on an Mx3005P real-time PCR system (Stratagene, CA, USA) using the Brilliant SYBR green master mix kit (Stratagene) and the primers listed in Table S1. The manufacturer's instructions were followed with the modification that the total reaction volume was reduced to 25 µl. Three technical replications were conducted for each sample. All qRT-PCR reactions were performed as follows: pre-incubation at 95 °C for 10 s, followed by 40 cycles of 95 °C for 30 s and 60 °C for 30 s. Following each reaction, the PCR products were subjected to melting-curve analysis, and representative samples were analyzed using electrophoresis to verify that only a single product was present. No template-negative controls were included with each set of reactions. The standard curve of each gene was confirmed to be in a linear range with the normalizing gene, elongation factor 1α (EF1α) ($r^2 > 0.98$). The expression level of the gene of interest (normalized to EF1α) is given relative to the corresponding control group with efficiency correction (Livak and Schmittgen 2001). EF1α expression remained constant across time. The efficiencies for primer pairs for NHE1, NHE2, NHE3, CFTR and EF1α were 96, 95.4, 97.1, 93.9 and 96.5, respectively. For comparisons among treatments (SW and HSW) and time points, the mRNA expression level of selected genes was calculated relative to the appropriate control group.

Plasma pH, ion concentrations, and osmolality

Blood pH was analyzed using a custom-built gas-tight, thermostatted sleeve equipped with a pH electrode (Radiometer pHc4000-8) attached to a MeterLab portable pH meter (Radiometer PHM201). Plasma total CO_2 was determined using a Corning 965 total CO_2 analyzer. Plasma pCO_2 and bicarbonate in blood plasma for acute transferred, cannulated fish were calculated from total CO_2 and pH according to the Henderson–Hasselbach equation using the appropriate toadfish plasma constants. More specifically, the HCO_3^- concentration was determined from Eq. (1) (Boutilier et al. 1984), while pCO_2 was determined from Eq. (2), using a pK_1 of 6.02 (apparent pK_1 for ionic strength of teleost plasma at 20 °C (Boutilier et al. 1984) and pK_2 of 9.46 for toadfish blood and intestinal fluids (Wilson and Grosell 2003; Wilson et al. 2002), αCO_2 of 0.038.

$$\left[HCO_3^-\right] = \left[\text{total } CO_2\right] / \left(1 + 10^{pH-pK_2}\right), \quad (1)$$

$$\left[\text{Molecular } CO_2\right] = \left[HCO_3^-\right] / \left(\alpha CO_{2*}\left(1 + 10^{pH-pK_1}\right)\right). \quad (2)$$

Plasma osmolality was analyzed by a Wescor 5520 vapor pressure osmometer.

Immunohistochemistry

After fixation in Z-fix for 48 h, an established protocol (Ruhr et al. 2014) was modified to prepare the tissues for immunofluorescence analysis. Gill tissues were immersed in 70% ethanol for 1 week. Tissues were then dehydrated in ascending grades of ethanol (3 washes in 95%, followed by 3 washes in 100%). Following dehydration, tissues were prepared for wax embedding by immersing them in two washes of butanol, followed by two washes with Histochoice (Amresco). Tissues were finally immersed in four washes of paraplast (McCormick Scientific) and embedded. Serial sections (4 µm) were cut from the tissues using a Leitz microtome (model 1512). Sections were transferred and mounted onto poly-L-lysine-coated slides and dried for 24 h at 37 °C. Slides were then prepared for antibody treatment by immersing them into two washes of Histochoice

(Amresco), five washes of decreasing alcohol (100%–50% ethanol), and one wash in PBS. Subsequently, slides were incubated in 10 mmol/l citric acid solution and placed in a microwave for two 5-min incubations for additional antigen retrieval. Slides were then immersed in 0.01% Tween-20 in PBS, followed by immersion in a 5% skim milk solution, and three washes in PBS. The primary antibody was dissolved in 0.5% skim milk in PBS, added to each slide, and incubated for 1 h at 37 °C. The primary antibody consisted of monoclonal mouse VHA (VHA B1/2) antibody (Santa Cruz Biotechnology, Inc., catalog number: sc-271832) which has a 96.6% identity to the corresponding toadfish sequence. After the 1-h incubation, slides were immersed in three PBS washes. The secondary antibodies consisted of Alexa flour 488-conjugated anti-mouse IgG (Invitrogen). Slides were once again incubated in 37 °C for 1 h, followed by three successive washes in PBS. Coverslips were placed on the slides using histology mounting medium with DAPI (Sigma F6057) to stain nuclei. Control slides were treated equally, but without primary antibody. Slides were observed with an Olympus fluorescence microscope (u-tvo.5xc-2), with attached QImaging camera (Retiga EXi, Fast 1394). iVision and Fiji software were used to analyze images. To examine possible VHA translocation, the slides stained with VHA B1/2 were observed with an Olympus confocal laser scanning biological microscope (FV1000).

Transmission electron microscopy

The whole gill arch was excised from the fish and then cut into pairs of filaments attached by the septum of the arch. The filaments were then post-fixed in a mixture of the glutaraldehyde fixative and osmium tetroxide (to make a 1% OsO_4 solution). This was followed by ten rinses in PBS buffer to remove the OsO_4/glutaraldehyde mixture. Tissue was dehydrated through three changes each in a graded series of ethanol (20%, 50%, 70%, 95%, 100%), then placed in two rinses of propylene oxide (Electron Microscopy Sciences, Hatfield, PA, USA) for 5 min each and then embedded in EPON resin and 1 µm semi-thin toluidine-stained sections cut to ascertain orientation. Thin sections were then cut with an ultramicrotome fitted with a diamond knife and stained with lead citrate and uranyl acetate. Sections were viewed and images taken at selected magnifications in a Philips CM-10 Electron Microscope fitted with a Gatan digital camera.

To detect potential changes in the percentage of mitochondria-rich cells (MRCs) with apical crypts, the number of MRCs and MRCs with apical crypt per lamellae were quantified. This was done by analyzing micrographs taken at a magnification of 3400X from at least three randomly selected lamellae per fish on three fish per treatment. Mean MRC surface area was determined by tracing the MRC perimeters using a morphometric software program (Fiji). Apical width was determined as the longest line along the apical surface. Apical depth was determined by drawing and measuring a line between the deepest point of apical crypt and apical opening edge.

Western blot analysis

Frozen gill samples were weighed, immersed in liquid nitrogen, and pulverized in an ice-cold porcelain grinder. The resultant powder was resuspended in 1:10 w/v of ice-cold homogenization buffer [250 mmol/l sucrose, 1 mmol/l EDTA, 30 mmol/l Tris, 10 µl/ml Halt™ Protease Inhibitor Cocktail (Life Sciences), pH 7.4] and needle sonicated on ice for 20 s. The homogenate was then subjected to differential centrifugation according to the procedure of Tresguerres et al. (2006). Briefly, debris was removed by low-speed centrifugation (3000*g* for 10·min, 4 °C), and a sample of the supernatant (whole gill homogenate) was stored at − 80 °C. The rest of the sample was then subjected to a medium speed centrifugation (20,800*g* for 60·min, 4 °C), and the pellet was resuspended in homogenization buffer and stored at − 80 °C as the plasma membrane fraction.

Samples of both the whole gill and gill membrane fractions were saved for protein concentration analysis via the bicinchoninic acid (BCA) method (Pierce, Rockford, IL, USA), which was performed in triplicate. The gill samples were then diluted with SDS loading buffer to a final concentration of 1 µg/µl. Twenty µg of total protein per sample was separated on a 4–20% polyacrylamide gradient mini-gel (45 min at 120 V; Bio-Rad Laboratories Inc., Hercules, CA, USA) and transferred to a PVDF membrane (45 min at 80 V) using a wet transfer cell (Bio-Rad Laboratories). Following blocking (protein-free blocking buffer: Thermo 37570), the PVDF membranes were incubated with the primary antibody against VHA, NKA, or CFTR with gentle agitation at 4 °C overnight. The NKA-α antibody was a commercial polyclonal rabbit Na^+/K^+-ATPase α antibody (sc-28800, Santa Cruz Biotechnology), which showed a sequence identity of 93% to the corresponding toadfish sequence. The affinity-purified H^+ pump antibody was developed in rabbits against a synthetic peptide based on the B subunit of eel V-H^+-ATPase (VHA) with sequence RKDHADVSNQLYACYA, which showed 100% identity to the corresponding toadfish sequence [a gift from Prof. Jonathan Wilson, (Wilson et al. 2007)]. The CFTR antibody was a commercial monoclonal mouse CFTR (R&D Systems, catalog number: MAB25031). After three washes of 15 min each with TBS-Tween 20 (0.05%), the PVDF membrane was incubated with horse-radish peroxidase (HRP)-conjugated secondary antibodies (Santa Cruz Biotechnology), at room temperature for 60 min. Blots were developed in WesternSure ECL substrate (Li-Cor), visualized via a C-DiGit chemiluminescent western blot scanner (Li-Cor, Inc.), and the relevant bands were quantified in Image Studio Lite (Li-Cor). Following

visualization, protein loading in each lane was quantified by staining with Coomassie Brilliant Blue and the relevant bands were normalized to a constant loading rate for comparison across treatments. The control (SW) and hypersaline (HSW) treatments were run on the same gel at the same time to ensure complete comparability. The abundance of the selected protein was calculated relative to the appropriate control group.

To confirm the specificity of the eel anti-VHA-B antibody, identical aliquots of whole gill lysates were run side by side on an SDS-PAGE gel. Half of the gel was then transferred to a PVDF membrane for western blotting using the VHA-B, while the second half was Coomassie stained. Upon completion of blotting, a band was cut from the Coomassie-stained gel at the molecular weight expected for VHA-B. The gel fragment was then submitted to trypsin digestion and the resulting peptides were analyzed by liquid chromatography-coupled mass spectrometry (LC–MS). Raw data were searched against a recently generated Gulf toadfish transcriptome (Schauer et al. 2016) translated into all six possible reading frames. The VHA-B was identified in this analysis with 47% sequence coverage. The eel VHA-B antibody cross reacted with a number of other proteins of different molecular weight and was therefore not used for immunohistochemistry. Immunohistochemistry of VHA was complete using a monoclonal mouse the VHA B1/2(sc-271832) antibody, which is very specific according to our western blot verification (Fig. S1).

Statistical analysis

Data are presented as absolute mean ± SE. Statistically significant difference of blood pH, plasma pCO_2, HCO_3^- concentrations and osmolality post-transfer from the 0 h and among treatments at each time point were revealed by a two-way ANOVAs, followed by multiple sample comparisons using the Holm–Sidak method. Statistically significant differences of quantitative analysis of V–H^+-ATPase subunit B, CFTR and NKA-α, quantitative analysis of MRCs in the lamellae of Gulf toadfish exposed to HSW compared to controls (S24 or S96) were revealed by *t* tests ($p \leq 0.05$). All *t* tests are two-tailed unless stated otherwise. Means were considered significantly different when $p < 0.05$. SAS9.3 (SAS Institute, Cary) was used for statistical analysis. Line and bar charts were created using Sigmaplot 11.0 (Systat Software, San Jose, CA).

Results

Blood acid–base status during salinity transfer

The blood pH of fish subjected to control SW (35 ppt) remained constant throughout the 96-h experiment, but transfer to 60-ppt seawater (HSW) induced a biphasic metabolic acidosis (Fig. 1a). Initially blood pH significantly decreased, which was followed by recovery at 2 h after the initiation of HSW exposure; however, from 4 to 96 h of HSW exposure, blood pH remained significantly suppressed (Fig. 1a). In HCO_3^--free, 60-ppt seawater (UHSW), the initial acidosis was more pronounced than in HSW, whereas it was virtually absent when 60-ppt water was buffered by HEPES (BHSW) (Fig. 1a). With exception of a lower level at 24 h, plasma [HCO_3^-] remained stable in control fish throughout the 96-h experiment (Fig. 1c). In contrast, plasma [HCO_3^-] of fish held in HSW and BHSW showed a steady decline for the first 24 h, followed by recovery to control levels. Fish held in UHSW displayed a gradual increase in plasma [HCO_3^-], reaching statistical significance by 72-h post-transfer (Fig. 1c). Plasma pCO_2 remained constant in control fish, but showed slight, yet significant, reductions in HSW and BHSW during the first 24 h following transfer (Fig. 1b). In contrast, fish in UHSW showed elevated plasma pCO_2 at 30 min post-transfer and throughout most of the remaining 96-h exposure. The plasma osmolality of all fish exposed to any of the 60-ppt treatments increased from 24 to 96 h post-transfer, while the control fish osmolality remained constant (Fig. 1d). The survival rates of toadfish during control, HSW, UHSW and BHSW transfer were 100%.

mRNA expression of acid–base and osmoregulation-relevant proteins

The mRNA expression of NHE1, NHE2, NHE3, and CFTR remained unchanged in the gills of toadfish during 7-d exposure to HSW (Table 2).

VHA, CFTR, and NKA abundance

Western blot analysis for VHA-B, CFTR, and NKA-α revealed distinct bands of ~ 48, ~ 135, and ~ 113 kDa, respectively. Chemical-fluorescence analysis (Fig. 2) on the whole gill homogenates (Fig. 2b) and isolated cytosolic fraction (Fig. 2c) showed no significant difference in VHA-B and CFTR abundance between treatments. However, in the isolated gill membrane fraction (Fig. 2a), a significant increase in VHA-B and NKA-α abundance in HSW treatment was found. Membrane VHA-B abundances in HSW treatments were sixfold ($p < 0.05$) and ninefold higher than control by 24- and 96-h post-transfer, respectively. NKA-α abundance in the membrane fraction increased by 1.7-fold after 96 h. NKA-α abundance in the whole-gill homogenates was also significantly higher in HSW treatments than control.

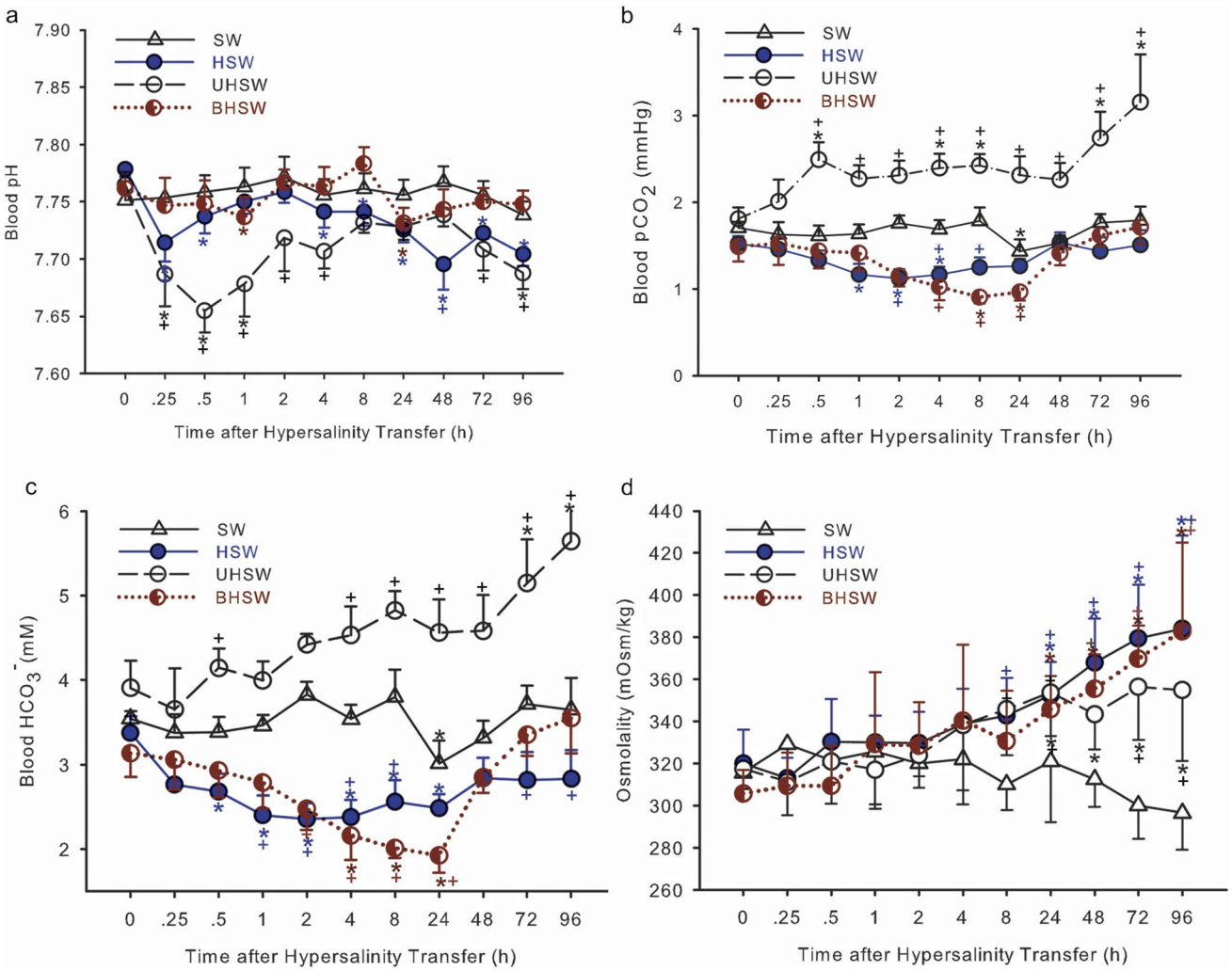

Fig. 1 Blood pH (**a**), pCO_2 (**b**) HCO_3^- concentrations (**c**) and osmolality (**d**) of Gulf toadfish acutely transferred from seawater (SW) to hypersaline water (60-ppt HSW, 60-ppt HCO_3^--free UHSW, 60-ppt HEPES-buffered HCO_3^--free BHSW) and sampled at 0-, 0.25-, 0.5-, 1-, 2-, 4-, 8-, 24-, 48-, 72-, and 96-h post-transfer. Values are mean ± SE ($N \geq 6$). Statistically significant difference between the pre-treatment (*0-h) and subsequent time points within the same treatment are represented with a *. Significant differences between treatments compared to control SW at each time point are represented with a "+". These differences were revealed by a two-way ANOVA tests, followed by multiple comparisons with Holm–Sidak method ($p \leq 0.05$). For statistical comparisons of all individual data points, please see table S2

Table 2 Relative mRNA expression of Na^+–H^+-exchanger 1, 2, 3 (NHE1, NHE2, NHE3) and CFTR in gill of Gulf toadfish acutely transferred from seawater (SW) to 60-ppt hypersaline water (HSW) and sampled at 0, 6-, 12-, 24-, 96- and 168-h post-transfer

Time (h)	0	6	12	24	96	168
NHE1	1.00 ± 0.17	0.99 ± 0.18	0.98 ± 0.17	0.99 ± 0.17	0.94 ± 0.11	1.00 ± 0.14
NHE2	0.99 ± 0.24	0.90 ± 0.15	0.84 ± 0.09	1.27 ± 0.45	1.38 ± 0.58	0.99 ± 0.10
NHE3	1.00 ± 0.24	0.99 ± 0.31	0.87 ± 0.13	1.18 ± 0.38	1.15 ± 0.30	1.00 ± 0.11
CFTR	1.00 ± 0.11	1.03 ± 0.14	1.12 ± 0.24	1.05 ± 0.20	1.00 ± 0.12	1.00 ± 0.13

Values are mean ± SE ($n \geq 5$)

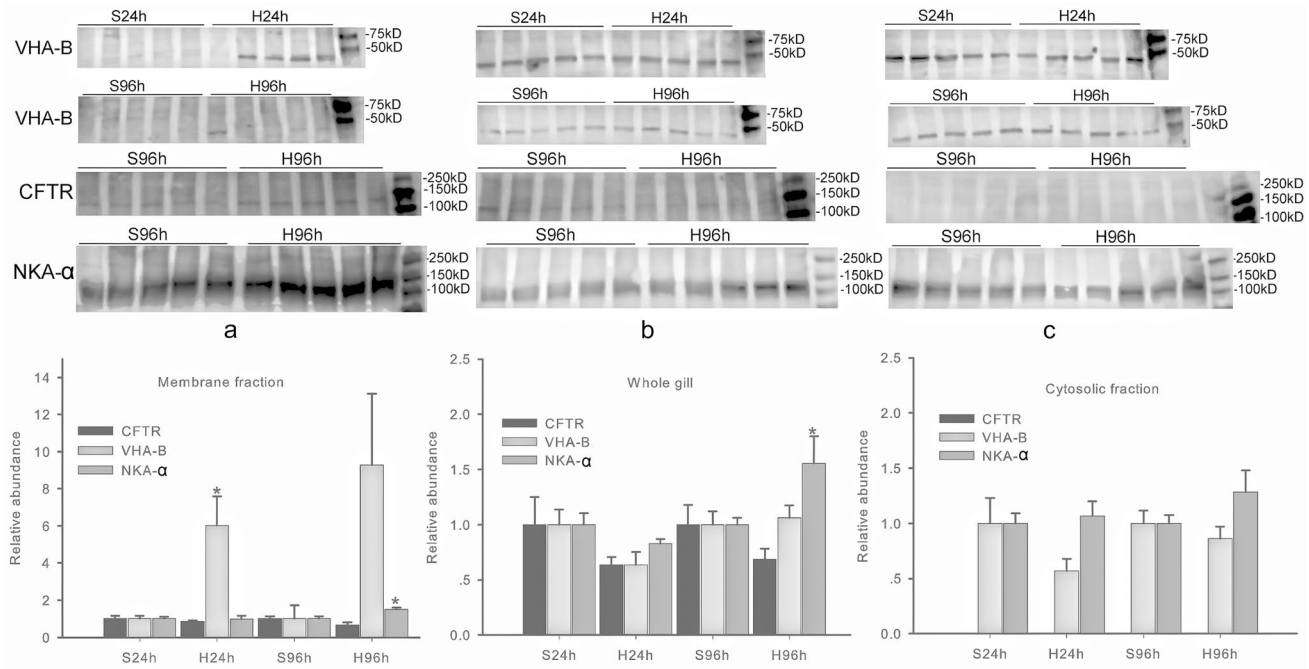

Fig. 2 Quantitative protein analysis of V-H$^+$-ATPase subunit B, CFTR, and NKA-α in gills from fish exposed to control seawater (SW; S24: 24-h exposure, S96: 96-h exposure) or 60-ppt hypersaline water (HSW; H24: 24-h exposure, H96: 96-h exposure) fish ($N=5$ per treatment). **a** Membrane fraction, **b** whole gill homogenates, **c** cytoplasm fraction. Representative immunoblots are shown above each panel. Statistically significant difference from corresponding control group (S24 or S96) were revealed by a pairwise *t* tests ($p \leq 0.05$) and indicated by asterisks (*). The affinity-purified H$^+$-pump antibody was developed in rabbits against a synthetic peptide based on the B subunit of eel V-H$^+$-ATPase (VHA) with sequence RKDHADVSNQLYACYA, a highly conserved sequence among V-H$^+$-ATPases (a gift from Prof. Jonathan Wilson, Wilfred Laurier University)

Transmission electron microscopic observations

In both SW and HSW, MRCs (characterized by a rich population of mitochondria and extensive tubular system in the cytoplasm) were found distributed along the lamellae. The apical crypts of MRCs in HSW were more clearly defined than in SW (Fig. 3). Although not quantified, there appears to be an enhanced tubular network in the cytoplasm in hypersaline treatment (Fig. 3e, f). Although no differences of the number of MRCs were found, the fraction of cells with apical crypts were significantly higher in HSW than SW (Fig. 4a). In addition, the width and depths of the apical crypts were greater in HSW than in SW fish (Fig. 4b).

Immunocytochemistry of VHA on lamellae

Western blot verification for VHA-B1/2 (Santa Cruz, sc-271832) revealed a single specific band of ~ 54 kD (Fig. S1). VHA localization in Gulf toadfish gills was observed by single staining. In lamellae, intense VHA immunoreactivity was detected in what appears to be MRCs (as shown in transmission electron microscopic photos) in both SW and HSW (Fig. 5).

Colchicine treatment

Following treatment with colchicine, blood pH (Fig. 6a) decreased more ($p=0.0355$, two-way ANOVA analysis for pH between HSW and HSW-Col) than in controls during the first 2 h after transfer to HSW with an apparent increase of plasma pCO_2 (Fig. 6b) and no apparent difference in plasma HCO_3^- (Fig. 6c) between the two groups.

Discussion

Fish compensate for elevated salinity and a transient acidosis by a variety of mechanisms that include one or more of four possible pathways, such as uptake or excretion of HCO_3^-, regulation of proton transport via Na^+/H^+ exchangers or translocation of proton pumps. The present study reveals a metabolic acidosis, defined by reduced pH in the absence of a rise in pCO_2, and an apparent compensatory branchial acid excretion in Gulf toadfish following transfer to elevated salinity. Increased net branchial acid excretion was inferred from blood pH differences among treatment groups. Although we cannot rule out a role for reduced HCO_3^- excretion, increased abundance of VHA in branchial

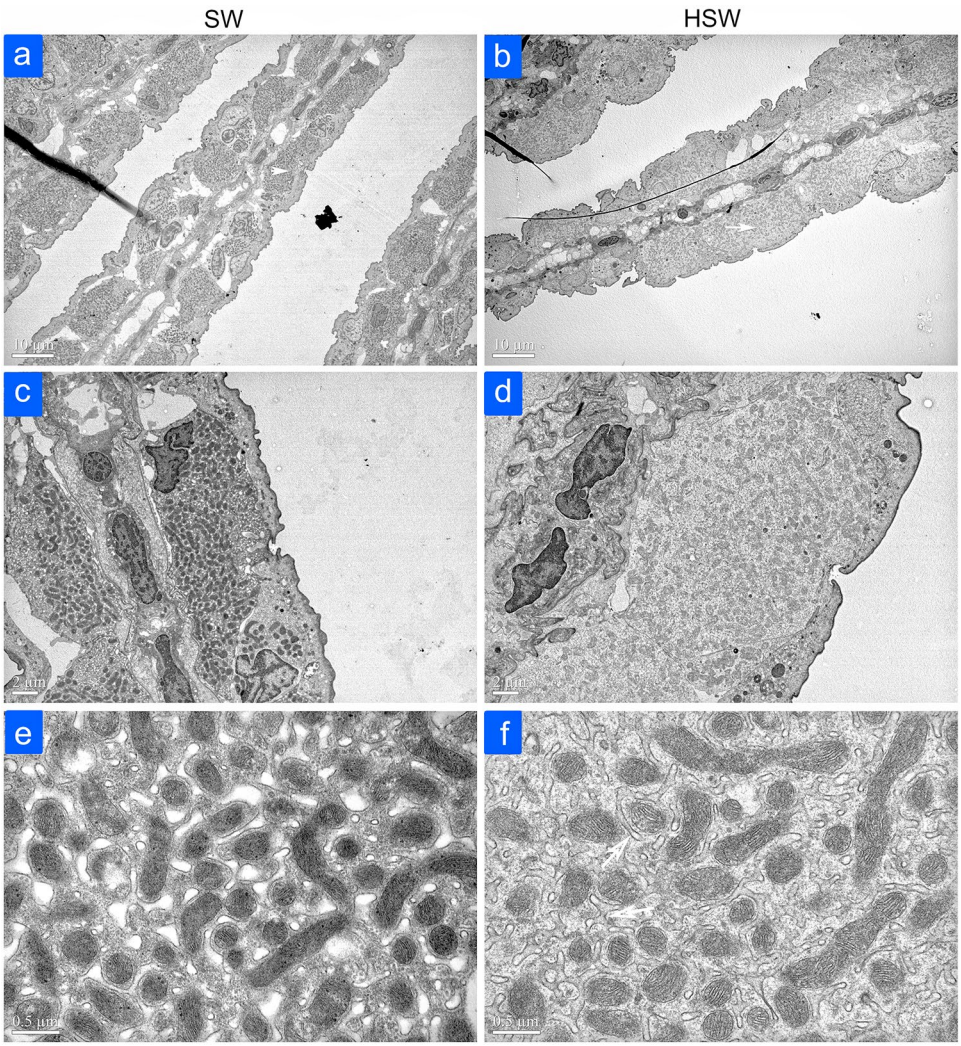

Fig. 3 Representative transmission electron micrographs of gill lamellar epithelia of Gulf toadfish, acutely transferred to control seawater (SW; 35 ppt; **a**, **c**, **e**) and hypersaline seawater (HSW; 60 ppt; **b**, **d**, **f**), for 96 h. Solid arrows indicate emergent mitochondria-rich cells (MRCs); asterisks (*) indicate apical crypts; an open arrow marks an example of tubular network

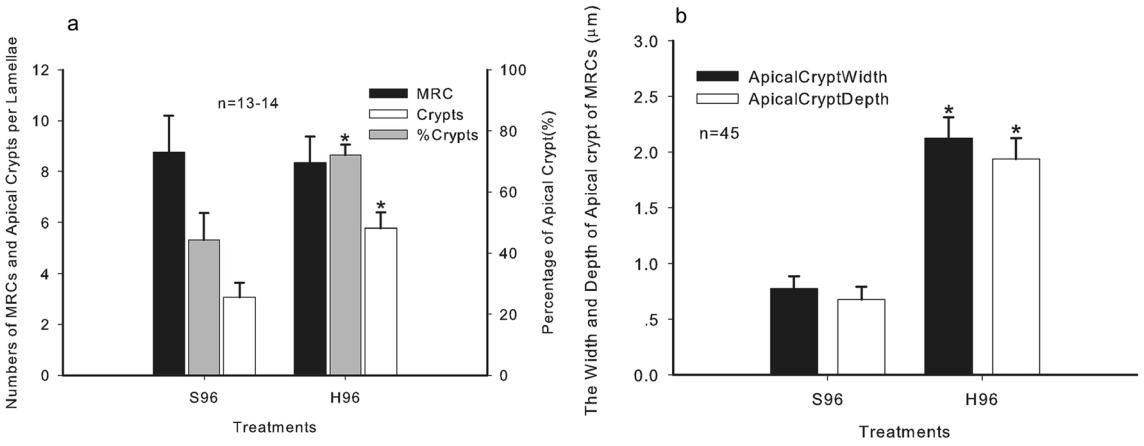

Fig. 4 Quantitative analysis of mitochondria-rich cells (MRCs) in the lamellae of Gulf toadfish exposed to control seawater (35 ppt) or hypersaline water (60 ppt), for 96 h (S96: 96-h exposure to control seawater; H96: 96-h exposure to 60 ppt). Statistically significant difference from corresponding control groups (S24 or S96) were revealed by pairwise *t* tests ($p \leq 0.05$) and indicated by asterisks (*)

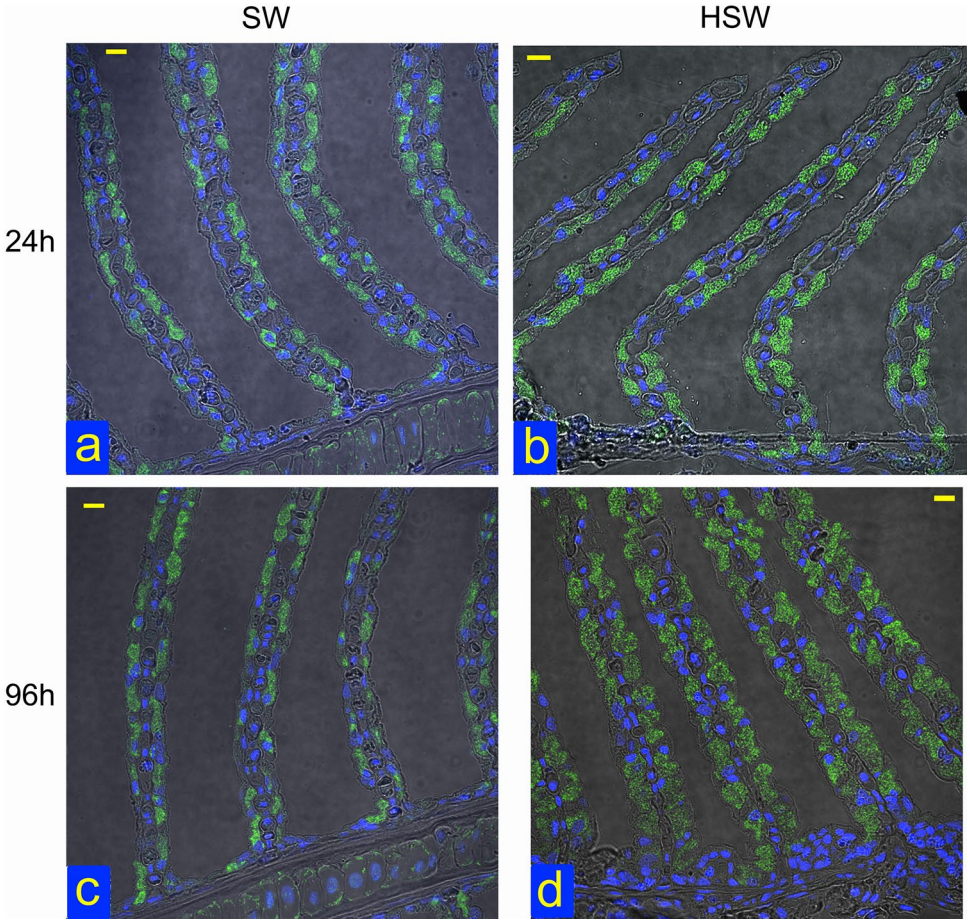

Fig. 5 Fluorescence images of VHA (green) immunoreactivity in gill lamella of Gulf toadfish exposed to control seawater (SW; 35 ppt) (**a**) for 24 h and (**c**) for 96 h, and to hypersaline water (HSW; 60 ppt) (**b**) for 24 h and (**d**) for 96 h; the images were overlaid with corresponding phase contrast. Scale bars, 10 µm. VHA antibody for Immunohistochemistry was monoclonal mouse VHA (VHA B1/2) antibody (SANTA CRUZ BIOTECHNOLOGY, INC., catalog number: sc-271832). The blue fluorescence is nuclear staining

cell membrane fractions may suggest H^+ excretion as compensation for the metabolic acidosis, which is achieved in part by VHA translocation to facilitate acid excretion. The suggestion of a role for translocation of H^+ transporters in compensation for metabolic acidosis following exposure to elevated salinity is supported by observations of reduced pH compensation following treatment with colchicine. Although we cannot rule out that NHEs and anion exchangers play a role in correcting the metabolic acidosis following exposure to elevated salinity, we provide evidence here that the proton pump may contribute to acid excretion.

Acidosis and compensation during hypersaline treatment

As expected, a transient metabolic acidosis was found when Gulf toadfish were acutely exposed to the 60-ppt, hypersaline seawater (HSW). This acidosis likely stems from the elevated intestinal secretion of HCO_3^- seen at higher salinities, and a delayed compensation by the gill that eventually increases net acid excretion in Gulf toadfish (Genz et al. 2008). The significance of osmoregulatory acid loading from the intestinal cells to the blood has also been illustrated in European flounder (Cooper et al. 2010). The experiments carried out in the present study tested whether this compensatory response was mediated by uptake of ambient HCO_3^- across the gill. Initial experiments with UHSW revealed not only a more pronounced acidosis, but also an increase in both plasma [HCO_3^-] and blood pCO_2, suggesting that unbuffered seawater may interfere with CO_2 excretion across the gill. It is possible that the boundary layer at the gills of fish held in UHSW was more acidic, slowing the conversion of molecular CO_2 to HCO_3^-, thus resulting in a less favorable partial pressure gradients for CO_2 excretion. Consequently, experiments were repeated with BHSW (HEPES-buffered) that revealed only minor disturbances of toadfish blood pH, as well as a transient drop in plasma [HCO_3^-] that was similar to what was observed in fish transferred to HSW. Based on these observations, we conclude that toadfish respond to the metabolic acid load associated with an increased osmoregulatory demand by either excreting acid or reducing HCO_3^- excretion rather than absorbing HCO_3^-. HCO_3^- uptake from 60-ppt water which contained 4.2 mM HCO_3^- as compared to 3–3.5 mM in the blood plasma would be possible considering mildly blood-side positive transepithelial potential of toadfish

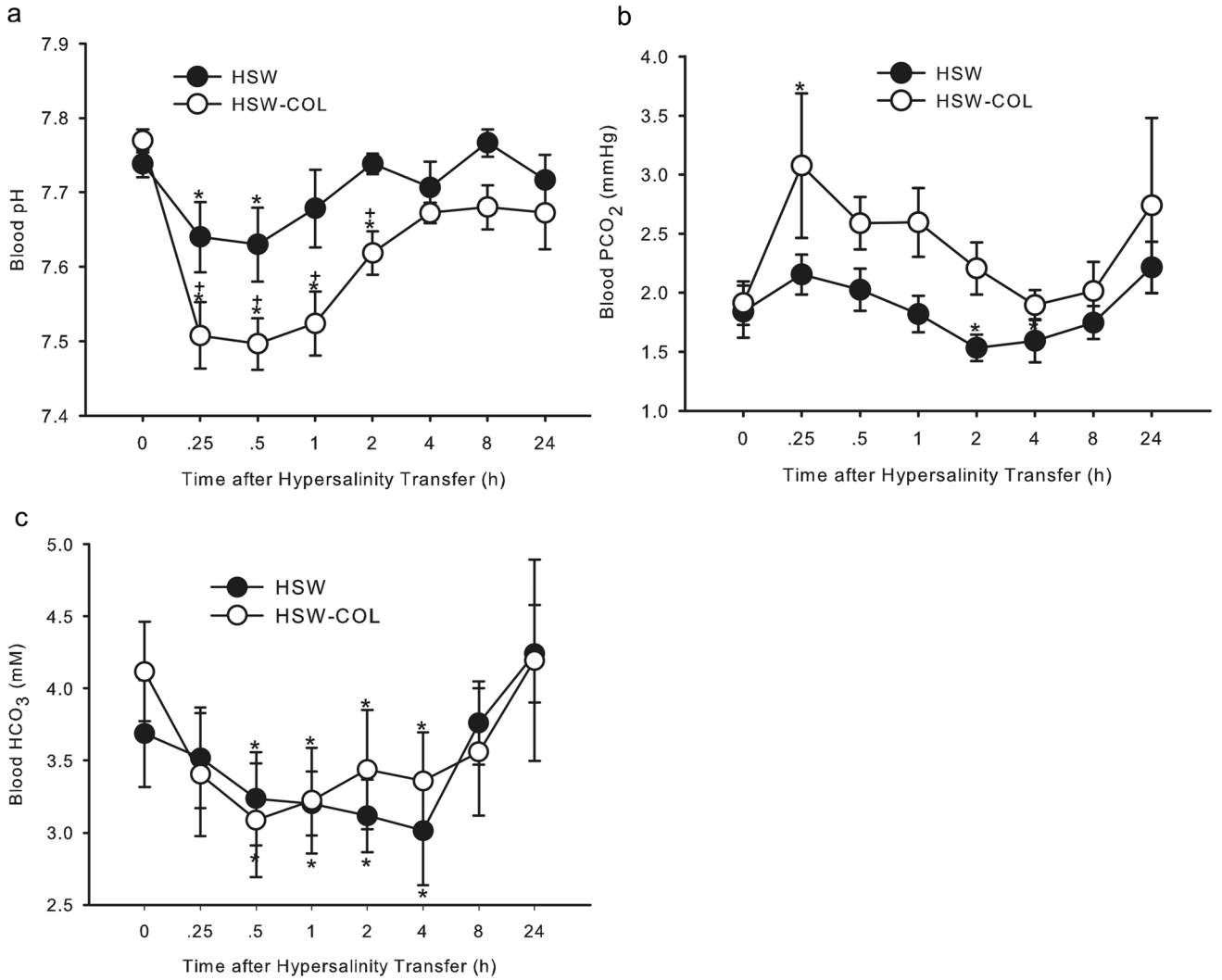

Fig. 6 Blood pH (**a**), plasma pCO_2 (**b**), and HCO_3^- concentration (**c**) of Gulf toadfish acutely transferred from seawater (SW) to 60-ppt (HSW) or colchicine-treated 60-ppt hypersaline water (HSW-COL), sampled at 0-, 0.25-, 0.5-, 1-, 2-, 4-, 8-, and 24-h post-transfer. Values are mean ± SE ($N \geq 6$). Statistically significant difference from the 0 h (*) and among treatments at each time point ("+"shows the significant different from HSW) were revealed by two-way ANOVA tests, followed by multiple comparisons with Holm–Sidak method ($p \leq 0.05$). For statistical comparisons of all individual data points. Please see Table S3

(Wood and Grosell 2008). Further, the presence of several anion exchangers (Esbaugh et al. 2012), of which at least one is electrogenic (Grosell et al. 2009b), and the electrogenic NBC1 (Taylor et al. 2010) in the toadfish gill tissue, combined with high substrate promiscuity of many anion exchangers (Mount and Romero, 2004) means that the possibility of transepithelial HCO_3^- uptake cannot be excluded. However, although HCO_3^- uptake may be possible, it does not appear to play a role in adjusting the metabolic acidosis observed in the present study. While several branchial acid excretion pathways are known (Brauner et al. 2019; Perry and Gilmour 2006), much less is known about HCO_3^- transport across gills of marine fish. Respiratory acidosis have in some cases been associated with upregulation of presumably basolateral AE1 isoforms (Tseng et al. 2013) as well as upregulation of basolateral SCL4a4 (NBC1) isoforms (Deigweiher et al. 2008; Tseng et al. 2013), but these responses are not consistent across species (Brauner et al. 2019). To our knowledge, even less is known about apical events that may contribute to HCO_3^- uptake. The conclusion of the present study, concerning a metabolic acidosis, distinguishes itself from an earlier study on Gulf toadfish, which suggested uptake of ambient HCO_3^- to compensate for a respiratory acidosis, induced by elevated ambient pCO_2 (Esbaugh et al. 2012). These divergent acid–base regulatory responses to a metabolic and a respiratory acidosis might suggest that Gulf toadfish are capable of sensing both extracellular pH and pCO_2. It is well established that teleost fish

are capable of sensing pCO_2 via branchial neuroepithelial cells (NECs) and that elevated pCO_2 results in depressed intracellular pH (pH_i) and inhibition of K^+ channels that leads to membrane depolarization and a rise in intracellular Ca^{2+} in these cells (Abdallah et al. 2015; Qin et al. 2010). Since several categories of K^+ channels are likely present in NECs, and some appear to respond to extracellular pH rather than pH_i [reviewed in (Perry and Tzaneva 2016)], it is possible that NECs are also sensors of extracellular pH and mediate the response to metabolic acidosis observed in the present study. However, this is speculative and remains to be studied.

Having established that Gulf toadfish do not rely on HCO_3^- uptake for compensation of a metabolic acidosis, we examined the possible roles of the VHA and NHEs. Our results revealed no significant changes in mRNA expression of NHEs, during a detailed time course following a 7-d transfer to hypersaline water. Although we cannot eliminate the possibility that NHE protein levels and their subcellular distribution changed during HSW acclimation, the lack of mRNA expression changes may suggest that NHEs are not major contributors to the observed compensatory response to the metabolic acidosis. Likewise, earlier studies of Gulf toadfish ruled out a role for transcriptional regulation of branchial VHA (whole gill, the membrane and cytoplasm were mixed), as well as whole gill homogenate VHA activity, as responsible for observed increases in branchial acid excretion following transfer to elevated salinity (Guffey et al. 2011).

VHA translocation might play an important role in the process of proton excretion

We found some evidence that translocation of VHA may play a role in the compensation for a metabolic acidosis that is induced by transfer to elevated salinity. The observed increase of VHA abundance in the gill membrane fraction indicates translocation of VHA during hypersaline treatment as a possible mechanism for increased acid secretion. This interpretation is further supported by our experiments on intact animals, during which application of colchicine, a microtubular network disrupter, resulted in a more pronounced acidosis following transfer from 35- to 60-ppt seawater. However, no clear evidence for translocation was observed by immunohistochemistry (Fig. 5) and, further, we have no evidence for translocation to the apical rather than the basolateral membrane, since the membrane isolation technique used does not distinguish between the two. However, VHA appears highly abundant in MRCs and it seems feasible that smaller changes in subcellular distribution, as indicated by the higher VHA abundance in the gill membrane fraction, may go undetected by immunohistochemistry.

In studies on elasmobranchs, VHA translocation from the cytoplasm to the basolateral membrane acts to enhance HCO_3^- secretion to combat induced alkalosis (Roa et al. 2014). Thus, there appears to be agreement between the present study on Gulf toadfish and the earlier studies on elasmobranchs with respect to a role for VHA translocation in acid–base balance regulation. However, Gulf toadfish subjected to a metabolic acidosis experience an apparent increased acid excretion, which would require the translocation of VHA to be to the apical region, whereas elasmobranchs show translocation to the basolateral membrane for acid retention during an alkalosis. We are unaware of reports of apical translocation of VHA but note that several freshwater fish and amphibians as well as marine fish and invertebrates show apical VHA localization in ion transporting epithelia (Grosell et al. 2009a, b; Guffey et al. 2011; Ip et al. 2018; Jensen et al. 1997; Larsen et al. 1992; Lin and Randall 1991; Lin et al. 2006).

Morphological changes of the chloride cell might promote the relocation of proton pumps

Deeper apical crypts and enhanced tubular network (Evans et al. 2005) in MRCs of 60-ppt-exposed fish may promote the relocation of transporters. Although no differences in the number of MRCs were found, the fraction of cells with apical crypts was significantly higher in HSW than SW (Fig. 4a) and these crypts were wider and deeper (Fig. 4b). It is unknown if these morphological changes observed after transfer to 60 ppt serve CFTR's function to accommodate the need for additional Cl^- excretion, function of acid–base transporters (and possible translocation to maintain acid–base balance), or both.

Conclusion

The present study reveals that metabolic acidosis, induced by exposure to elevated ambient salinity, is not compensated by HCO_3^- uptake. Inhibition of this compensation by colchicine, and increased abundance of VHA in membrane fractions of gill cells, may suggest a role for VHA translocation in enhanced H^+ excretion, although apical translocation has yet to be demonstrated. Earlier work by our group has shown that branchial mRNA expression of cytosolic carbonic anhydrase (CAc) (Sattin et al. 2010) and Na^+–K^+-ATPase (NKA) (Guffey et al. 2011) is upregulated by elevated salinity. Increased CAc likely catalyzes the conversion of CO_2 to H^+ and HCO_3^- to aid in acid–base regulation, whereas NKA is upregulated to support additional ion excretion. A transient metabolic acidosis was seen in the present and three earlier studies (Maxime et al. 1991; Nonnotte and Truchot 1990; Wilkes and McMahon 1986),

of fish transferred to higher salinities. Translocation of a transporter, as suggested by the current study, rather than de novo synthesis may represent a faster and less energetically demanding response to rapidly fluctuating and high salinities as encountered by Gulf toadfish in their natural environment (Kelble et al. 2007). Finally, differential compensatory strategies to cope with the salinity-induced metabolic acidosis (lack of HCO_3^- uptake) in the present study and a CO_2-induced respiratory acidosis (HCO_3^- uptake) in previous work (Esbaugh et al. 2012) in the same species illustrate that regulatory strategies vary depending on environmental variables. Future studies ought to include attempts to isolate apical membranes of marine teleost fish gills for detection of VHA presence and activity. This study adds to the growing literature of how a model marine teleost copes with perturbations to acid–base balance.

Acknowledgements We thank Drs. M. Danielle McDonald and Michael C. Schmale, from the Rosenstiel School of Marine and Atmospheric Science, for the generous use of their equipment, and Patricia Blackwelder, at the University of Miami Center for Advanced Microscopy, for her assistance with electron microscopy.

Author contributions ZY and MG conception and design of research; ZY, KLS, IMR, EMM, and RMH: performed experiments; ZY and MG: analyzed data; ZY and MG: interpreted the results of the experiments; ZY: prepared figures; ZY: drafted manuscript; ZY, KLS, IMR, EMM, RMH and MG: edited and revised manuscript; M.G.: approved the final version of the manuscript.

Funding This work was supported by a National Science Foundation (USA) award (1146695) and Central Public-interest Scientific Institution Basal Research Fund (China), CAFS (NO. 2017GH13). MG is a Maytag Chair of Ichthyology.

Compliance with ethical standards

Conflict of interest No conflicts of interest, financial or otherwise, are declared by the authors.

References

Abdallah SJ, Jonz MG, Perry SF (2015) Extracellular H^+ induce Ca^{2+} signals in respiratory chemoreceptors of zebrafish. Eur J Physiol 467:399–413. https://doi.org/10.1007/s00424-014-1514-2

Bath RN, Eddy FB (1979) Ionic and respiratory regulation in rainbow-trout during rapid transfer to seawater. J Comp Physiol B 134(4):351–357. https://doi.org/10.1007/bf00710003

Boutilier RG, Heming TA, Iwama GK (1984) Physiochemical parameters for use in fish respiratory physiology. In: Hoar WS, Randa DJ (eds) Fish Physiology, vol X(A). Academic Press, Orlando, pp 403–427

Brauner CJ, Shartau RB, Damsgaard C, Esbaugh AJ, Wilson RW, Grosell M (2019) Acid-base physiology and CO_2 homeostasis: regulation and compensation in response to elevated environmental CO_2. In: Grosell M, Munday PL, Farrell AP, Braune CJ (eds) Carbon dioxide. Fish Physiology, vol 37, pp 69–132

Catches JS, Burns JM, Edwards SL, Claiborne JB (2006) Na^+/H^+ antiporter, V-H^+-ATPase and Na^+/K^+-ATPase immunolocalization in a marine teleost (*Myoxocephalus octodecemspinosus*). J Exp Biol 209:3440–3447. https://doi.org/10.1242/jeb.02384

Claiborne JB, Edwards SL, Morrison-Shetlar AI (2002) Acid-base regulation in fishes: cellular and molecular mechanisms. J Exp Zool 293:302–319. https://doi.org/10.1002/jez.10125

Cooper CA, Whittamore JM, Wilson RW (2010) Ca^{2+}-driven intestinal HCO_3^- secretion and $CaCO_3$ precipitation in the European flounder in vivo: influences on acid–base regulation and blood gas transport. Am J Physiol Regul Integr Comp Physiol 298:R870–R876. https://doi.org/10.1152/ajpregu.00513.2009

Deigweiher K, Koschnick N, Portner HO, Lucassen M (2008) Acclimation of ion regulatory capacities in gills of marine fish under environmental hypercapnia. Am J Physiol Regul Integr Comp Physiol 295(5):R1660–R1670. https://doi.org/10.1152/ajpregu.90403.2008

Esbaugh AJ, Perry SF, Bayaa M, Georgalis T, Nickerson J, Tufts BL, Gilmour KM (2005) Cytoplasmic carbonic anhydrase isozymes in rainbow trout *Oncorhynchus mykiss*: comparative physiology and molecular evolution. J Exp Biol 208:1951–1961. https://doi.org/10.1242/jeb.01551

Esbaugh AJ, Heuer R, Grosell M (2012) Impacts of ocean acidification on respiratory gas exchange and acid–base balance in a marine teleost, *Opsanus beta*. J Comp Physiol B 182:921–934. https://doi.org/10.1007/s00360-012-0668-5

Evans DH, Piermarini PM, Choe KP (2005) The multifunctional fish gill: dominant site of gas exchange, osmoregulation, acid–base regulation, and excretion of nitrogenous waste. Physiol Rev 85:97–177. https://doi.org/10.1152/physrev.00050.2003

Genz J, Taylor JR, Grosell M (2008) Effects of salinity on intestinal bicarbonate secretion and compensatory regulation of acid–base balance in *Opsanus beta*. J Exp Biol 211:2327–2335. https://doi.org/10.1242/jeb.016832

Gilmour KM, Perry SF, Wood CM, Henry RP, Laurent P, Part P, Walsh PJ (1998) Nitrogen excretion and the cardiorespiratory physiology of the gulf toadfish, *Opsanus beta*. Physiol Zool 71:492–505

Gonzalez RJ (2012) The physiology of hyper-salinity tolerance in teleost fish: a review. J Comp Physiol B 182:321–329. https://doi.org/10.1007/s00360-011-0624-9

Grosell M (2006) Intestinal anion exchange in marine fish osmoregulation. J Exp Biol 209:2813–2827. https://doi.org/10.1242/jeb.02345

Grosell M (2010) The role of the gastrointestinal tract in salt and water balance. In: Grosell M, Farrell AP, Brauner CJ (eds) The multifunctional gut of fish. Fish Physiology, vol 30, pp 136–156. https://doi.org/10.1016/S1546-5098(10)03004-9

Grosell M (2011) Intestinal anion exchange in marine teleosts is involved in osmoregulation and contributes to the oceanic inorganic carbon cycle. Acta Physiol (Oxf) 202:421–434. https://doi.org/10.1111/j.1748-1716.2010.02241.x

Grosell M, Taylor JR (2007) Intestinal anion exchange in teleost water balance. Comp Biochem Physiol A: Mol Integr Physiol 148:14–22. https://doi.org/10.1016/j.cbpa.2006.10.017

Grosell M, Gen J, Taylor JR, Perry SF, Gilmour KM (2009a) The involvement of H^+-ATPase and carbonic anhydrase in intestinal HCO_3^- secretion on seawater-acclimated rainbow trout. J Exp Biol 212:1940–1948. https://doi.org/10.1242/jeb.026856

Grosell M, Mager EM, Williams C, Taylor JR (2009b) High rates of HCO_3^- secretion and Cl^- absorption against adverse gradients in the marine teleost intestine: the involvement of an electrogenic anion exchanger and H^+-pump metabolon? J Exp Biol 212(Pt 11):1684–1696. https://doi.org/10.1242/jeb.027730

Guffey S, Esbaugh A, Grosell M (2011) Regulation of apical H^+-ATPase activity and intestinal HCO_3^- secretion in marine

fish osmoregulation. Am J Physiol Regul Integr Comp Physiol 301:R1682–R1691. https://doi.org/10.1152/ajpregu.00059.2011

Ip YK, Hiong KC, Lim LJY, Choo CYL, Boo MV, Wong WP, Neo ML, Chew SF (2018) Molecular characterization, light-dependent expression, and cellular localization of a host vacuolar-type H^+-ATPase (VHA) subunit A in the giant clam, Tridacne squamosa, indicate the involvement of the host VHA in the uptake of inorganic carbon and its supply to the symbiotic zooxanthellae. Gene 659:137–148. https://doi.org/10.1016/j.gene.2018.03.054

Jensen LJ, Sørensen JB, Hviid LE, Willumsen NJ (1997) Proton pump activity of mitochondria-rich cells, the interpretation of external proton-concentration gradients. J Gen Physiol 109:73–91. https://doi.org/10.1085/jgp.109.1.73

Kelble CR, Johns EM, Nuttl WK, Lee TN, Smith RH, Ortner PB (2007) Salinity patterns of Florida Bay. Estuar Coast Shelf Sci 71:318–334

Kurita Y, Nakada TN, Kato A, Doi H, Mistry AC, Chang M, Romero MF, Hirose S (2008) Identification of intestinal bicarbonate transporters involved in formation of carbonate precipitates to stimulate water absorption in marine teleost fish. Am J Physiol Regul Integr Comp Physiol 294:R1402–R1412. https://doi.org/10.1152/ajpregu.00759.2007

Larsen EH, Willumsen NJ, Christoffersen BC (1992) Role of proton pump of mitochondria-rich cells for active-transport of chloride-ions in toad skin epithelium. J Physiol Lond 450:203–216. https://doi.org/10.1113/jphysiol.1992.sp01912

Larsen EH, Deaton LE, Onken H, O'Donnell M, Grosell M, Dantzler WH, Weihrauch D (2014) Osmoregulation and excretion. Compr Physiol 4:405–573. https://doi.org/10.1002/cphy.c130004

Lin H, Randall D (1991) Evidence for the presence of an electrogenic proton pump on the trout gill epithelium. J Exp Biol 61:119–134

Lin LY, Horng JL, Kunkel JG, Hwang PP (2006) Proton pump-rich cell secretes acid in skin of zebrafish larvae. Am J Physiol Cell Physiol 290(2):C371–C378. https://doi.org/10.1152/ajpcell.00281.2005

Liu ST, Tsung L, Horng JL, Lin LY (2013) Proton-facilitated ammonia excretion by ionocytes of medaka (*Oryzias latipes*) acclimated to seawater. Am J Physiol Regul Integr Comp Physiol 305:R242–R251. https://doi.org/10.1152/ajpregu.00047.2013

Liu ST, Horng JL, Chen PY, Hwang PP, Lin LY (2016) Salt secretion is linked to acid–base regulation of ionocytes in seawater-acclimated medaka: new insights into the salt-secreting mechanism. Sci Rep 6:31433. https://doi.org/10.1038/srep31433

Livak KJ, Schmittgen TD (2001) Analysis of relative gene expression data using real-time quantitative PCR and the $2^{-\Delta\Delta CT}$ method. Methods 25:402–408. https://doi.org/10.1006/meth.2001.1262

Maxime V, Pennec J, Peyraud C (1991) Effects of direct transfer from freshwater to seawater on respiratory and circulatory variables and acid–base status in rainbow trout. J Comp Physiol [B] 161:557–568

Milne RS, Randall DJ (1976) Regulation of arterial pH during freshwater to sea-water transfer in rainbow-trout salmo-gairdneri. Comp Biochem Physiol A Physiol 53(2):157–160. https://doi.org/10.1016/s0300-9629(76)80047-3

Mount DB, Romero MF (2004) The SLC26 gene family of multifunctional anion exchangers. Pflug Archiv Eur J Physiol 447:710–721. https://doi.org/10.1007/s00424-003-1090-3

Nonnotte G, Truchot J (1990) Time course of extracellular acid–base adjustments under hypo- or hyperosmotic conditions in the euryhaline fish *Platichthys flesus*. J Fish Biol 36:181–190

Perry SF, Gilmour KM (2006) Acid-base balance and CO_2 excretion in fish: unanswered questions and emerging models. Respir Physiol Neurobiol 154(1–2):199–215. https://doi.org/10.1016/j.resp.2006.04.010

Perry SF, Hemin TA (1981) Blood ionic and acid–base status in rainbow-trout (*salmo-gairdneri)* following rapid transfer from freshwater to seawater—effect of pseudobranch denervation. Can J Zool 59(6):1126–1132. https://doi.org/10.1139/z81-157

Perry SF, Tzaneva V (2016) The sensing of respiratory gases in fish: mechanisms and signalling pathways. Respir Physiol Neurobiol 224:71–79. https://doi.org/10.1016/j.resp.2015.06.007

Qin Z, Lewis JE, Perry SF (2010) Zebrafish (*Danio rerio*) gill neuroepithelial cells are sensitive chemoreceptors for environmental CO_2. J Physiol 588:861–872. https://doi.org/10.1113/jphysiol.2009.184739

Roa JN, Munevar CL, Tresguerres M (2014) Feeding induces translocation of vacuolar proton ATPase and pendrin to the membrane of leopard shark (*Triakis semifasciata*) mitochondrion-rich gill cells. Comp Biochem Physiol A: Mol Integr Physiol 174:29–37. https://doi.org/10.1016/j.cbpa.2014.04.003

Ruhr IM, Bodinier C, Mager EM, Esbaugh AJ, Williams C, Takei Y, Grosell M (2014) Guanylin peptides regulate electrolyte and fluid transport in the Gulf toadfish (*Opsanus beta*) posterior intestine. Am J Physiol Regul Integr Comp Physiol 307:R1167–R1179. https://doi.org/10.1152/ajpregu.00188.2014

Ruiz-Jarabo I, Gregorio SF, Gaetano P, Trischitta F, Fuentes J (2017) High rates of intestinal bicarbonate secretion in seawater tilapia (*Oreochromis mossambicus*). Comp Biochem Physiol A Mol Integr Physiol 207:57–64. https://doi.org/10.1016/j.cbpa.2017.02.022

Sattin G, Mager EM, Beltramini M, Grosell M (2010) Cytosolic carbonic anhydrase in the Gulf toadfish is important for tolerance to hypersalinity. Comp Biochem Physiol A Mol Integr Physiol 156:169–175. https://doi.org/10.1016/j.cbpa.2010.01.018

Schauer KL, LeMoine CM, Pelin A, Corradi N, Warren WC, Grosell M, McDonald MD (2016) A proteinaceous organic matrix regulates carbonate mineral production in the marine teleost intestine. Sci Rep 6:34494. https://doi.org/10.1038/srep34494

Taylor JR, Mager EM, Grosell M (2010) Basolateral NBCe1 plays a rate-limiting role in transepithelial intestinal HCO_3^- secretion, contributing to marine fish osmoregulation. J Exp Biol 213:459–468. https://doi.org/10.1242/jeb.029363

Tresguerres M, Parks SK, Katoh F, Goss GG (2006) Microtubule-dependent relocation of branchial V-H^+-ATPase to the basolateral membrane in the Pacific spiny dogfish (*Squalus acanthias*): a role in base secretion. J Exp Biol 209:599–609. https://doi.org/10.1242/jeb.02059

Tseng YC, Hu MY, Stumpp M, Lin Y, Melzner F, Hwang PP (2013) CO_2-driven seawater acidification differentially affects development and molecular plasticity along life history of fish (*Oryzias latipes*). Comp Biochem Physiol A Mol Integr Physiol 165(2):119–130. https://doi.org/10.1016/j.cbpa.2013.02.005

Wilkes PRH, Mcmahon BR (1986) Responses of a stenohaline freshwater teleost (*Catostomus commersoni*) to hypersaline exposure. J Exp Biol 121:77–94

Wilson RW, Grosell M (2003) Intestinal bicarbonate secretion in marine teleost fish-source of bicarbonate, pH sensitivity, and consequences for whole animal acid–base and calcium homeostasis. Biochim Biophys Acta 1618:163–174. https://doi.org/10.1016/j.bbamem.2003.09.014

Wilson RW, Wilson JM, Grosell M (2002) Intestinal bicarbonate secretion by marine teleost fish–why and how? Biochim Biophys Acta 1566:182–193. https://doi.org/10.1016/s0005-2736(02)00600-4

Wilson JM, Leitão A, Gonçalves AF, Ferreira C, Reis-Santos P, Fonseca A, da Silva J, Antunes JC, Pereira-Wilson C, Coimbra J (2007) Modulation of branchial ion transport protein expression by salinity in glass eels (*Anguilla anguilla* L.). Mar Biol 151:1633–1645. https://doi.org/10.1007/s00227-006-0579-7

Wood CM, Grosell MA (2008) Critical analysis of transepithelial potential in intact killifish (*Fundulus heteroclitus*) subjected to acute and chronic changes in salinity. J Comp Physiol B 178(6):713–727. https://doi.org/10.1007/s00360-008-0260-1